Oxygen-vacancy-induced charge redistribution in the CuO_2 planes of non-stoichiometric $RBa_2Cu_3O_{7-x}$ (0<x<1) determined by neutron crystal-field spectroscopy

1989 J. Phys.: Condens. Matter 1 3715

(http://iopscience.iop.org/0953-8984/1/23/018)

J. Phys.: Condens. Matter **1** (1989) 3715–3720. Printed in the UK

LETTER TO THE EDITOR

Oxygen-vacancy-induced charge redistribution in the CuO_2 planes of non-stoichiometric $RBa_2Cu_3O_{7-x}$ ($0 < x < 1$) determined by neutron crystal-field spectroscopy

Albert Furrer and Peter Allenspach

Laboratorium für Neutronenstreuung, Eidgenössische Technische Hochschule Zürich, CH-5303 Würenlingen, Switzerland

Received 10 March 1989

Abstract. Neutron crystal-field spectroscopy as a probe of the local symmetry at the rare-earth site in non-stoichiometric $RBa_2Cu_3O_{7-x}$ ($0 < x < 1$) is introduced. The oxygen vacancy concentration x induces charge redistributions that are modelled by virtual distortions of the oxygen ordering in the CuO_2 planes. The model assumptions are quantitatively accounted for by neutron spectroscopic data obtained for $HoBa_2Cu_3O_{7-x}$ ($x = 0.2, 0.8$). Some implications of the observed charge redistributions on the superconducting properties are discussed.

It has been realised that the oxygen stoichiometry and oxygen defect structure are crucial quantities determining the occurrence or disappearance of superconductivity in the perovskite-type compounds $RBa_2Cu_3O_{7-x}$ (R denotes yttrium and most rare earths). A myriad of diffraction experiments (see, for example, [1]) established the main features of the oxygen ordering, which are often found to depend strongly upon the preparation conditions. For $x = 0$ the structure consists of two CuO_2 planes and one CuO_3 chain per unit cell as shown in figure 1. As x increases, the planes remain intact, while oxygen vacancies appear in the chains. At $x = 1$, the structure comprises intact planes and isolated CuO_2 units (empty chains). The crystallographic symmetry changes from orthorhombic to tetragonal at $x = 0.6$. The lattice parameters change almost linearly up to $x = 0.5$; for $0.5 < x < 0.6$ the orthorhombicity rapidly converges towards $b/a = 1$ and a step-like increase in c occurs. The superconductivity exhibits a two-plateau structure of T_c versus x (see, for example, [2]). $T_c = 90$ K superconductivity is found for $0 \leqslant x \leqslant 0.2$. T_c then decreases to 60 K, where it remains up to $x = 0.5$. For $x > 0.5$ the superconductivity deteriorates and is completely lost above $x = 0.6$. While the disappearance of superconductivity correlates almost exactly with the rapid change of the lattice parameters at $0.5 < x < 0.6$, the jump of T_c from 90 K to 60 K at $0.2 < x < 0.3$ cannot be reconciled with the available structural data. In this Letter we introduce a model that describes the effect of the removal of oxygen from the chains in terms of charge redistributions in the CuO_2 planes. The R^{3+} ions are sandwiched between the CuO_2 planes (see figure 1) and thus constitute local probes that are susceptible to these charge redistributions through the crystalline-electric-field (CEF) potential experienced by the 4f electrons. These charge redistributions have actually been observed in neutron

0953-8984/89/233715 + 06 $02.50

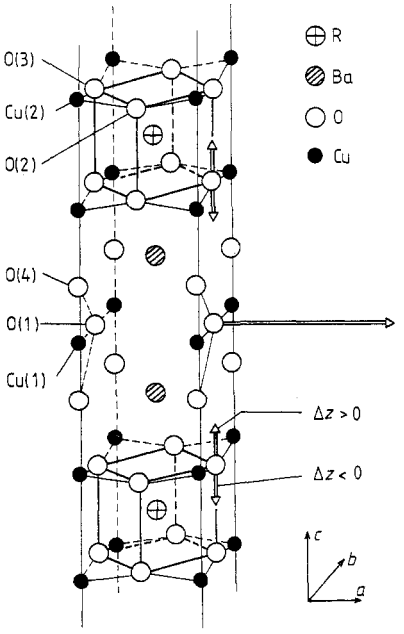

Figure 1. The structure of $RBa_2Cu_3O_{7-x}$. The removal of an O(1) atom and the proposed virtual rearrangement of the O(3) atoms is indicated by arrows.

spectroscopic experiments on $HoBa_2Cu_3O_{7-x}$ [3, 4] which will be quantitatively analysed. It is this charge redistribution that presumably results both in the two-plateau structure of T_c and in the final loss of superconductivity with increasing x.

The removal of an oxygen O(1) atom from the chain in orthorhombic $RBa_2Cu_3O_{7-x}$ causes some structural relaxation around the vacancy which, according to single-crystal x-ray diffraction [5], is quite pronounced for the structural layer containing the Cu(1) site and its neighbouring oxygen sites, O(1) and O(4), whereas the superconducting CuO_2 layers remain almost undistorted by the relaxation mechanism. On the other hand, we expect a modification of the charge distribution of the superconducting CuO_2 planes close to the vacancy. This charge redistribution is likely to be more pronounced for atomic sites close to the O(1) vacancy than for the more distant sites, i.e., the charge distribution around the rare-earth sites close to the vacancy is expected to exhibit an anisotropy which in turn gives rise to a modification of the CEF potential

$$V(\boldsymbol{r}) = \sum_i q_i/|\boldsymbol{r} - \boldsymbol{R}_i| \tag{1}$$

where q_i and $\boldsymbol{R}_i$ denote the effective charge and position of the ith ligand ion, respectively. In actual calculations the anisotropy of the CEF potential can be taken into account by appropriately modifying the effective charges q_i of the respective neighbouring ligands, see equation (1).

In the present work we model the charge redistribution around the R^{3+} sites in a different manner. Recent inelastic neutron scattering (INS) experiments on orthorhombic $HoBa_2Cu_3O_{6.8}$ [3] and tetragonal $HoBa_2Cu_3O_{6.2}$ [4] provided evidence that the CEF potential $V(\boldsymbol{r})$ at the Ho^{3+} site is mainly determined by the charge distribution of the nearest-neighbouring oxygen shell. Therefore, according to equation (1) the anisotropy of the CEF potential introduced by the removal of an O(1) atom from the chain in

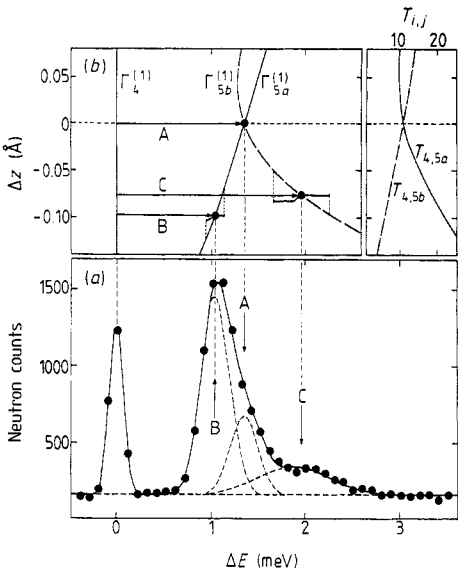

Figure 2. (*a*) Low-energy part of the CEF splitting pattern of $HoBa_2Cu_3O_{6.2}$ observed by neutron spectroscopy [4]. The curves are described in the text. $T = 1.5$ K, $Q = 1.1$ Å^{-1}. (*b*) Low-energy CEF states $|\Gamma_i\rangle$ and selected transition probabilities $T_{i,j}$ of Ho^{3+} in $HoBa_2Cu_3O_{6.2}$ versus virtual displacement Δz of a single O(3) atom.

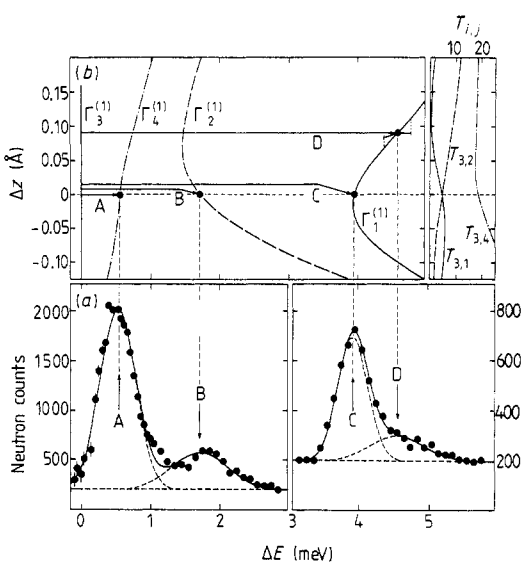

Figure 3. (*a*) Low-energy part of the CEF splitting pattern of $HoBa_2Cu_3O_{6.8}$ observed by neutron spectroscopy [3]. The elastic line is subtracted from the data. The curves are described in the text. $T = 1.5$ K, $Q = 1.1$ Å^{-1}. (*b*) Low-energy CEF states $|\Gamma_i\rangle$ and selected transition probabilities $T_{i,j}$ of Ho^{3+} in $HoBa_2Cu_3O_{6.8}$ versus virtual displacement Δz of a single O(3) atom.

orthorhombic $RBa_2Cu_3O_{7-x}$ can also be described by virtual displacements $\Delta \boldsymbol{R}_i$ of part of the nearest-neighbouring O(2) and O(3) ions out of their equilibrium positions $\boldsymbol{R}_i$. Moreover, in a first approximation the superposition principle of the CEF interaction allows us to model the charge redistribution by performing a virtual displacement of a single oxygen atom; thus we introduce a virtual displacement of the two O(3) atoms close to the O(1) vacancy along the z direction which either enhances or reduces the local R–O(3) distance as defined in figure 1 by $\Delta z > 0$ or $\Delta z < 0$, respectively, and thereby properly modifies the charge distribution of the CuO_2 planes. For geometrical reasons this virtual structural rearrangement of the O(3) atoms could equivalently involve the x direction, but not the y direction. In tetragonal $RBa_2Cu_3O_{7-x}$ the insertion of an O(1) atom into the chain produces a charge redistribution that can be modelled by a virtual rearrangement of the O(3) atoms (in tetragonal symmetry the O(2) and O(3) positions cannot be distinguished) in the opposite z direction.

The low-energy parts of the CEF spectra observed for orthorhombic $HoBa_2Cu_3O_{6.8}$ [3] and tetragonal $HoBa_2Cu_3O_{6.2}$ [4] are shown in figures 2(*a*) and 3(*a*). All the intensity was unambiguously proven to be of magnetic origin by a detailed study of the scattering against momentum transfer. Some of the CEF transitions exhibit a considerable asymmetry, namely the line at 1 meV for $HoBa_2Cu_3O_{6.2}$ and the line at 4 meV for $HoBa_2Cu_3O_{6.8}$. It is exactly this asymmetry of the peak shapes which carries the information on the charge redistributions of the CuO_2 planes as outlined below.

We have examined the energies of the CEF states $|\Gamma_i\rangle$ as well as the corresponding transition probabilities $T_{i,j} = |\langle\Gamma_j|J|\Gamma_i\rangle|^2$ upon virtually displacing a single O(3) atom out of its equilibrium position. The effect of this virtual distortion is to modify the geometrical

coordination factors through equation (1) and in turn to change the CEF splittings and transition probabilities as shown in figures 2(*b*) and 3(*b*). Both quantities exhibit a considerable dispersion versus Δz, and the results for $\Delta z > 0$ and $\Delta z < 0$ are drastically different, i.e., they allow us readily to discriminate between the two virtual distortional configurations. In our model $\Delta z < 0$ and $\Delta z > 0$ refer to a reduction and an enhancement of the negative charge densities associated with the O(3) sites, respectively.

Let us now consider the energy spectrum of $HoBa_2Cu_3O_{6.2}$ in detail. A least-squares fit to Gaussian peaks clearly gives rise to three inelastic lines as shown in figure 2(*a*). According to figure 2(*b*) the virtual displacement Δz splits the 'undistorted' singlet–doublet CEF transition $\Gamma_4^{(1)} \rightarrow \Gamma_5^{(1)}$ into two 'distorted' components $\Gamma_4^{(1)} \rightarrow \Gamma_{5a}^{(1)}$ and $\Gamma_4^{(1)} \rightarrow \Gamma_{5b}^{(1)}$. For reasonably moderate values of Δz the observed CEF splitting pattern can only be reproduced for $\Delta z < 0$, thus the line A can immediately be attributed to the 'undistorted' CEF transition, and the lines B and C correspond to the 'distorted' CEF excitations, which are indicated in figure 2(*b*) together with their intrinsic linewidths. We derive $\Delta z = -0.10 \pm 0.03$ Å and $\Delta z = -0.08 \pm 0.03$ Å for the lines B and C, respectively. An intensity comparison confirms our interpretation. For the intensity ratio of the peaks B and C we find $I_B/I_C = 2.7 \pm 0.7$, which is in good agreement with the calculated value $I_B/I_C = 3.2$. With $x = 0.8$ roughly two thirds of the Ho^{3+} ions experience the 'distorted' CEF interaction (the statistics of our model is described in detail in [6]), so the 'undistorted' CEF transition (peak A) can hardly be recognised in the observed energy spectrum, which may cause interpretation problems when deriving CEF parameters from the experimental data.

Similarly we performed a least-squares fit of the energy spectrum of $HoBa_2Cu_3O_{6.8}$ to Gaussian peaks as shown in figure 3(*a*). According to figure 3(*b*) the energies and intensities of the observed CEF splittings can only be reconciled with $\Delta z > 0$, which readily explains that resolution problems prevented the energy differences between the 'distorted' and 'undistorted' CEF transitions to show up clearly except for the $\Gamma_3^{(1)} \rightarrow \Gamma_1^{(1)}$ transition. Nevertheless, the lines A and B are considerably broader than the instrumental resolution, which indicates the presence of 'distorted' CEF transitions. In addition, they exhibit some fine structure in the range $1 < \Delta E < 1.5$ meV which may well be accounted for by our model, see figure 3(*b*). The 'distorted $\Gamma_3^{(1)} \rightarrow \Gamma_1^{(1)}$ transition is indicated in figure 3(*b*) together with its intrinsic line width, which results in a virtual displacement $\Delta z = +0.09 \pm 0.02$ Å. Again, with $x = 0.2$ the majority of the Ho^{3+} ions experience the 'distorted' CEF interaction [6] which, however, does not dominate the scattering because of its very small transition probability, see figure 3(*b*).

The signs of Δz as well as the sign reversal of Δz between tetragonal and orthorhombic $HoBa_2Cu_3O_{7-x}$ are consistent with our model, and the size of Δz is remarkably constant in both phases. Assuming a Gaussian distribution of the virtual displacements Δz,

$$g(\Delta z) \sim \exp[(\Delta z - \Delta z_0)^2/2\sigma^2] \tag{2}$$

we obtain $|\Delta z_0| = 0.09 \pm 0.02$ Å and $\sigma = 0.021 \pm 0.009$ Å. The mean virtual displacement Δz_0 is fairly well established and typically corresponds to a 10% change of the charge density at the O(3) sites. The variance σ, on the other hand, exhibits a considerable statistical uncertainty because of the limited energy resolution in the INS experiments [3, 4]. A more precise value of σ appears to be highly desirable in the light of recent electron diffraction experiments on $YBa_2Cu_3O_{6.5}$ that were interpreted in terms of a superstructure due to oxygen-vacancy ordering [7]. In principle neutron crystal-field spectroscopy should be susceptible to oxygen-vacancy ordering, since then the 'distorted' CEF transitions are expected to show up as narrow lines with $\sigma \rightarrow 0$

similar to the 'undistorted' CEF excitations. Although the presently available INS data on $HoBa_2Cu_3O_{7-x}$ slightly favour a statistical distribution of oxygen vacancies against oxygen-vacancy ordering, we have to await the results of high-resolution INS experiments in order to discriminate between the two cases conclusively.

We have quantitatively exemplified our model for the non-stoichiometric compounds $HoBa_2Cu_3O_{7-x}$ ($x = 0.2, 0.8$). Similar effects have also been observed in INS experiments on $NdBa_2Cu_3O_{6.86}$ [8], where even larger splittings of the CEF transitions induced by the oxygen vacancies were observed. On the other hand, recent INS experiments on stoichiometric $DyBa_2Cu_3O_{7.0}$ [9] gave no evidence for 'distorted' CEF excitations at all, in agreement with the physical picture of our model.

We now proceed to discuss the implications of the observed charge redistribution in the CuO_2 planes of $RBa_2Cu_3O_{7-x}$ versus oxygen-vacancy concentration x for the superconducting properties. According to our model calculations performed for $HoBa_2Cu_3O_{6.8}$ the removal of O(1) atoms causes charge redistributions that enhance the negative charge density at the O(3) sites by typically 10%. It is appealing to interpret this charge redistribution in terms of a mechanism that transfers electrons from the chains to the planes [10]. The net effect of this mechanism is to reduce the hole concentration in the planes, which is an important property in most theories of high-T_c superconductivity. Statistical considerations show that for $x = 0.25$ the majority of the CuO_2 planes are subject to this charge redistribution [6], and it is exactly the range $0.2 < x < 0.3$ where T_c rapidly decreases from 90 K to 60 K. A maximum disturbance of the charge distribution is reached for $x \simeq 0.6$ [6] where the superconductivity is lost, i.e., the suppression of superconductivity does not have to coincide with the orthorhombic-to-tetragonal phase transition as recently observed for $ErBa_2Cu_3O_{7-x}$ [11].

In conclusion, we have introduced the application of neutron spectroscopy to probe the local symmetry at the R site in non-stoichiometric $RBa_2Cu_3O_{7-x}$ through the observation of 'distorted' and 'undistorted' CEF excitations. We have interpreted the available neutron data for $HoBa_2Cu_3O_{7-x}$ in terms of charge redistributions modelled by virtual displacements of the oxygen O(3) atoms along the z axis. We feel that neutron crystal-field spectroscopy as a probe of local symmetry properties is a promising tool in further applications, similar to other local probes such as EXAFS and NMR measurements. The only condition is to be able to insert a rare-earth ion as a marker at the lattice site of interest. For example, in the recently synthesised high-T_c compounds of composition $R_{1+y}Ba_{2-y}Cu_3O_{7-x}$ that preserve superconductivity up to $y \simeq 0.4$ [12], excess R ions will substitute for deficient Ba sites where they experience a different charge distribution than at the original R site. Therefore, INS experiments on $R_{1+y}Ba_{2-y}Cu_3O_{7-x}$ ($0 < x < 1$) are expected to provide information on the charge redistribution at the O(4) sites that are closest to the O(1) vacancy, see figure 1.

We are indebted to Drs W Bührer and P Fischer for many helpful remarks and for critically reading the manuscript. We thank Dr H Heer for providing the computer program RESTA in the numerical calculations. Financial support by the Swiss National Science Foundation is gratefully acknowledged.

References

[1] Jorgensen J D, Beno M A, Hinks D G, Soderholm L, Volin K J, Hitterman R L, Grace J D, Schuller I K, Segre C U, Zhang K and Kleefisch M S 1987 *Phys. Rev.* B **36** 3608

[2] Cava R J, Batlogg B, Sunshine S A, Siegrist T, Fleming R M, Rabe K, Schneemeyer L F, Murphy D W,

van Dover R B, Callagher P K, Glarum S H, Nakahara S, Farrow R C, Krajewski J J, Zahurak S M, Waszczak J V, Marshall J H, Marsh P, Rupp L W Jr, Peck W F and Rietman E A 1988 *Physica* C **153–155** 560

[3] Furrer A, Brüesch P and Unternährer P 1988 *Phys. Rev.* B **38** 4616

[4] Allenspach P, Furrer A, Brüesch P, Marsolais R and Unternährer P 1989 *Physica* C **157** 58

[5] Schmahl W W, Salje E and Liang W Y 1988 *Phil. Mag. Lett.* **58** 173

[6] Allenspach P 1988 *Diploma Thesis* ETH Zürich

[7] Chaillout C, Alario-Franco M A, Capponi J J, Chenavas J, Strobel P and Marezio M 1988 *Solid State Commun.* **65** 283

[8] Allenspach P, Furrer A, Brüesch P and Unternährer P 1989 *Physica* B **156–157** 864

[9] Furrer A, Allenspach P and Hulliger F 1988 *J. Magn. Magn. Mater.* **76–77** 594

[10] Cava R J, Batlogg B, Rabe K M, Rietman E T, Gallagher P K and Rupp L W Jr 1988 *Physica* C **156** 523

[11] Maletta H, Pörschke E, Rupp B and Meuffels P unpublished

[12] Uwe H, Han T-S, Harada R and Sakudo T 1988 *Physica* C **153–155** 930